Journal of Particle Science and Technology 10 (2) (2024) 73-86

Iranian Research Organization for Science and Technology (IROST)

Journal of PARTICLE Science & Technology

JPSIT
https://jpst.irost.ir

Online ISSN: 2423-4079
Print ISSN: 2423-4087

Enhanced sulfate removal from aqueous solution using ion-exchanged clinoptilolite: A study on adsorption efficiency and process optimization

Saeideh Hematian , Kiana Peyvandi✉

Faculty of Chemical, Gas and Petroleum Engineering, Semnan University, Semnan, Iran

HIGHLIGHTS

- Clinoptilolite zeolite was prepared and adsorption experiments were carried out for sulfate removal from water.
- An efficient and economical process was introduced for ion exchange of clinoptilolite with high prospects for industrial applications.
- Response surface methodology (RSM) was used to optimize the parameters of modification.
- The modified clinoptilolite has an excellent removal effect on sulfate ions.

GRAPHICAL ABSTRACT

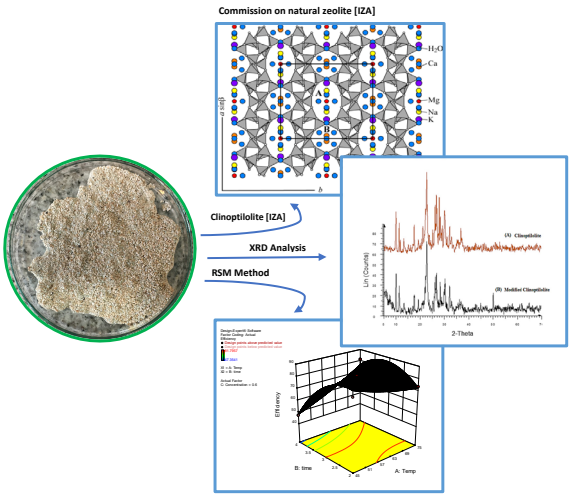

ARTICLE INFO

Article type:

Research article

Article history:

Received 27 September 2024
Received in revised form 6 November 2024
Accepted 13 November 2024

Keywords:

Clinoptilolite
Water treatment
Sulfate removal
Ion exchange
RSM method

DOI: 10.22104/jpst.2024.7130.1264

ABSTRACT

Zeolites such as clinoptilolite, a class of microporous crystalline materials, have gained significant attention thanks to their exceptional adsorption capabilities. This study explored the modification of clinoptilolite through an ion exchange process to boost its sulfate removal efficiency, a simple and cost-effective method. To optimize the adsorption process, the study evaluated the impact of temperature, time, and solution concentration on sulfate removal performance using the Response surface methodology (RSM). The results indicated that the maximum adsorption efficiency (81.79 %) was achieved at a temperature of 60 °C, a contact time of 3 h, and a solution concentration of 0.6 M. Characterization techniques, including X-ray diffraction (XRD), Fourier-transform infrared spectroscopy (FT-IR), and energy-dispersive X-ray spectroscopy (EDS) were employed to analyze the structural changes and performance of the modified clinoptilolite. Overall, this study demonstrates the potential of modified clinoptilolite as an effective and sustainable adsorbent for sulfate removal, offering promising prospects for industrial water treatment applications.

✉ *Corresponding author: E-mail address:* k_peyvandy@semnan.ac.ir ; *Tel:* +9831-533932

1. Introduction

Water is essential for human survival, supporting needs like drinking, hygiene, and household activities. Access to clean, affordable water is vital for health, helping to prevent dehydration, reduce pollution, and mitigate health risks [1]. However, most water sources are saline and unsuitable for consumption, and the scarcity of freshwater makes providing clean water challenging. Water's solvent properties, due to its polarity and ability to form hydrogen bonds, allow it to dissolve impurities, linking water quality to landscape changes, natural phenomena, and human activities. Water pollution occurs when substances or energy forms are introduced into a body of water, altering its composition and negatively impacting its intended use [2].

The increasing population and industrial activities have caused significant water contamination, creating a scarcity of clean water. This has led to the need for effective water treatment processes, including reusing water and treating wastewater, to address water shortages and ensure access to safe water [1]. Water treatment involves improving water quality and removing pollutants through various operations. Numerous methods exist to purify water for drinking or industrial reuse, targeting specific contaminants such as nitrates, sulfates, organic materials, and heavy metals. Sulfates, in particular, are a common water contaminant found near oil wells or in areas with sedimentary rocks. Agricultural practices using sulfate-containing fertilizers and industrial wastewater can also introduce sulfates into water sources [3].

Sulfate (SO_4^{2-}) is a prevalent contaminant in the sewage treatment industry and inorganic chemical production. It is commonly found as an impurity in salt brine used in the chlor-alkali industry [4,5]. Sulfate poses significant risks to both the environment and industrial processes. In addition to causing flaky layers in water pipes and an unpleasant taste, sulfate can lead to diarrhea in humans and animals and interfere with clothing washing [3,4]. Furthermore, sulfate can accumulate in salt brine circulation systems, elevating its concentration in electrolytic cells, reducing electrolytic current efficiency, and shortening the lifespan of expensive ion-exchange membranes.

In the mining industry, high sulfate concentrations in wastewater can accelerate equipment deterioration. Although sulfate is generally non-toxic, unlike heavy metals, it can disrupt the natural sulfur cycle when discharged in high concentrations. These issues have underscored the importance of removing harmful contaminants from water [3,5].

Various treatment methods are employed to remove sulfate ions (SO_4^{2-}) from water, including membrane separation, chemical precipitation, crystallization, ion exchange, biological treatment, electro-dialysis, and adsorption [5-7]. While each method has its merits and drawbacks, adsorption is often preferred due to its simplicity, low cost, and high efficiency.

Adsorption is a process that uses adsorbent materials to remove inorganic anions from aqueous solutions, particularly for sulfate removal from brine and industrial wastewater. Common adsorbents include activated carbon, alumina, ion-exchange resins, and metal-based materials, with specific ones like limestone, silica gel, and zirconia being used for sulfate removal [3,5,8,9]. Recent research has focused on creating new adsorbents with customizable surface chemistry to improve adsorption capacity and cost-effectiveness compared to traditional materials like synthetic resins. Materials such as metal-organic frameworks (MOFs) [10], graphene oxides [11], mesoporous silicas [12], biochars [13,14], metal oxides, and zeolites [15,16] have demonstrated exceptional capabilities in capturing inorganic anions from aqueous solutions.

Zeolites, hydrated aluminosilicates, are found in both natural and synthetic forms. Their three-dimensional structures, composed of silicon and aluminum atoms bonded by oxygen atoms in tetrahedral arrangements, create microporous channels and cavities [3]. As aluminosilicate minerals with interconnected cavities and a large surface area, zeolites are widely used in commercial applications as adsorbents and catalysts. Zeolite-based treatment methods are cost-effective, environmentally friendly, and highly effective in removing inorganic contaminants, including heavy metals, due to their exceptional contaminant adsorption capacity. To enhance their adsorptive performance and surface strength, chemical modifications using materials such as iron and manganese have been applied to zeolite surfaces [17,18].

Natural zeolites, porous, hydrated aluminosilicate minerals, exhibit valuable physicochemical properties, including sorption, molecular sieving, cation exchange, and catalysis. Their characteristics and widespread availability have made them a focal point of environmental research. Clinoptilolite, in particular, is the most common natural zeolite and is extensively used worldwide [19-22].

Recent research has focused on sulfate uptake using natural zeolites [23-30]. Hongqin Ma *et al.*, for example, examined spherical amorphous $ZrO(OH)_2$/AlOOH composite adsorbent beads for SO_4^{2-} removal from water. They found that the maximum adsorption capacity can reach 205 $mg.g^{-1}$ [5].

In another study, researchers explored the ion exchange process between surface hydroxyl groups and sulfate during the adsorption-desorption of sulfate using a $ZrO(OH)_2$/Y-zeolite adsorbent. Modifying Y-zeolite with zirconium enhanced the adsorbent's performance, resulting in high SO_4^{2-} adsorption capacity, selectivity, and regeneration efficiency [4]. Norapat Pratinthong *et al.* investigated optimal conditions for sulfate

removal from lignite coal mine drainage in Thailand using ettringite precipitation. They evaluated various operating conditions and achieved sulfate removal rates of 99.6 % and 99.0 % in both Lamphun and Lampang mine drainage under the optimized parameters [31].

Khabazipour *et al.* assessed the sulfate removal capabilities of hierarchical zeolitic imidazole framework 8 (H/ZIF-8) and its bimetallic derivatives, H/ZIF-8@La and H/ZIF-8@Cu. Kinetic modeling revealed that the removal reaction followed a pseudo-second-order mechanism [1].

Congli Qin *et al.* studied the effects of iron species on the simultaneous removal of nitrate and sulfate in artificial wetlands with varying COD concentrations [32]. Using Constructed wetland (CW) microcosms with low (100 $mg.L^{-1}$) and high (300 $mg.L^{-1}$) COD concentrations, they compared the performance of different groups, including CW-Con (with quartz sand), CW-ZVI (with quartz sand and zero-valent iron), etc. Under low COD conditions, the CW-ZVI group demonstrated superior nitrate and sulfate removal compared to the CW-Mag group. The CW-ZVI group achieved the highest removal rates for both nitrate (97.1 %) and sulfate (96.9 %).

As discussed previously, various adsorbents have been explored for pollutant removal. Adsorption methods offer a cost-effective and promising approach for water and wastewater treatment. Consequently, significant efforts have been invested in developing efficient water treatment solutions.

This study aimed to develop a simple, low-cost, and effective method for sulfate removal using natural zeolite. The method for removing sulfate from concentrated aqueous solutions was designed to be applicable in industry, where wastewater typically contains high levels of sulfate ions, a topic that has received less attention. Using an inexpensive, safe, and readily available NaCl solution, the cation exchange process, was employed to modify the zeolite structure and enhance its sulfate removal capacity. To optimize the process, three parameters (temperature, time, and solution concentration) were altered and examined using the Box-Behnken method. Some studies have been conducted on the processing of zeolite so far, but no research has been done on achieving optimal operational conditions in the ion exchange process, which is a highly important issue. The study successfully identified the most effective and cost-efficient conditions for sulfate uptake.

2. Experimental

2.1. Materials

Clinoptilolite, a zeolite with a high cation exchange capacity, was chosen for this study. The distribution of cations within a zeolite structure depends on factors such as size, charge, and coordination with the framework lattice or water molecules [33,34].

Clinoptilolite particles with a mesh size of 35 (particle size: 0.4-0.5 mm) were obtained from Afrazand Co. Ltd, Iran. The chemical formula for the clinoptilolite unit cell can be represented as $(X)_6(Al_6Si_{30}O_{72})\cdot 20H_2O$, where X represents exchangeable cations within the framework [33].

Sodium chloride ($NaCl \geq 99.9\%$), purchased from Merck Co. Ltd, Germany, was used as a cation exchange agent in solution form. Sodium sulfate ($Na_2SO_4 \geq 99\%$) was also purchased from Merck Co. Ltd, Germany, and served as the stock solution for sulfate introduction in this study.

2.2. Preparation of zeolite adsorbent

Ion exchange is a well-established phenomenon in crystalline materials, including minerals. Numerous experiments have demonstrated that various microporous minerals, across different chemical classes, can exchange cations with both diluted and pure salt solutions at ambient temperature. The ability of a crystalline material to exchange ions with an electrolyte without disrupting its crystal structure defines ion exchange. Over 500 minerals exhibit the structural characteristics necessary for ion exchange, including tube, layer, or framework-based structures with open channels [2]. Zeolites, a large group of crystalline materials, are particularly effective on ion exchange processes. Their adsorption capabilities are significantly enhanced through simple and cost-effective ion exchange modifications. This makes zeolites valuable for a wide range of applications [35-37].

In this study, clinoptilolite (NZ) particles were modified using an ion exchange method with NaCl solution. In the initial step, the clinoptilolite particles were thoroughly washed with distilled water to remove any residual dust. The particles were dried in an oven at 110 °C for 3 h in the second step.

In the third step, varying amounts of NaCl powder were used to prepare solutions with concentrations of 0.2, 0.6, and 1 M. Double-distilled water was used as the solvent for the ion exchange solution. An ultrasonic bath was employed to ensure the homogeneity of the solution. Then, a suspension containing 10 g of clinoptilolite (NZ) and 50 ml of NaCl solution was placed in a flat-bottomed flask and placed on a magnetic stirrer.

The experiments were conducted at various temperatures (45, 60, and 75 °C), contact times (2, 3, and 4 h), and NaCl solution concentrations (0.2, 0.6, and 1 M). The operating conditions were systematically varied to evaluate their impact on the adsorption process.

In the fourth step, the suspension was washed, filtered using

Whatman 42 filter paper, and dried in an oven at 60 °C for 3 h (Fig. 1). Lastly, a stock solution was prepared for conducting batch adsorption experiments. To prepare a stock solution containing sulfate ions, a specific amount of anhydrous sodium sulfate was added to a 250 ml volumetric flask, followed by the addition of double-distilled water to achieve a concentration of 0.1 M. A 250 ml glass beaker was utilized to assess the adsorption capacity of modified clinoptilolite (MNZ) for SO_4^{2-} from water. The test mixture consisted of 100 ml of aqueous Na_2SO_4 solution and approximately 1 g of adsorbent (on an absolute dry mass basis). The mixing speed in all experiments was maintained at 700-800 rpm. The residual sulfate ion concentration in the solution was determined using the ASTM D516 method and a spectrophotometer (DR 5000 Hach, USA). Samples containing sulfate ions were prepared according to ASTM D516 and analyzed at a wavelength of 420 nm to measure the remaining sulfate content. The experiments have been conducted based on the output table from the specialized design software. A brief explanation of this method is provided in the next section.

2.3. Experimental design

Design Expert 10 software was utilized for data analysis and statistical experimental design. The Box-Behnken design under Response Surface Methodology (RSM) was employed to optimize the three key variables in this study. Unlike whole or fractional factorial designs, Box-Behnken designs are centered at the center of each k-1 subarea of the experimental domain. Each factor is evaluated at three levels in these designs. Note that the Box-Behnken design for three factors does not meet the iso-variance per rotation criterion [38-42]. Design Expert software was utilized to generate an expert matrix for screening up to 50 factors. Analysis of variance (ANOVA) was employed to evaluate the statistical significance of these factors.

Response surface methodology (RSM) was used to quantify the relationship between the derived response surfaces and the controllable input parameters. RSM offers a more efficient process optimization approach than traditional one-factor-at-a-time methods, especially when dealing with experimental data. The Box-Behnken design, a statistical experimental technique, was used to identify optimal conditions for the desired formulation based on a limited number of experimental runs. These designs are not based on full or fractional factorial designs. The design points are positioned at the middle of the subareas of the dimension k-1. In the case of three factors, for instance, the points are located in the middle of the edges of the experimental domain. As reported in Table 1, the Box-Behnken tests utilized three levels: low (−1), central (0), and high (+1) [42].

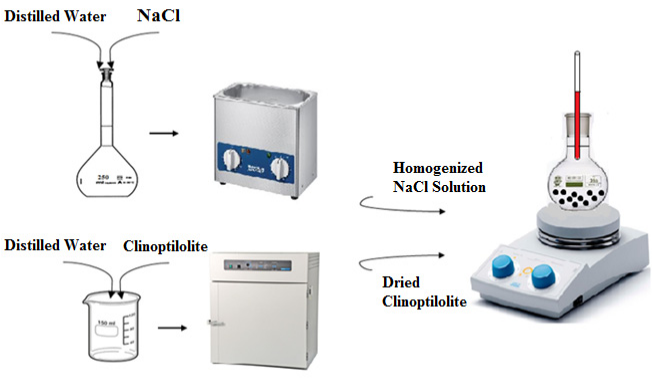

Fig. 1. Schematic diagram of the preparation of modified clinoptilolite.

Table 1. Levels of operating parameters.

Factor	Name	Units	Low (-1)	Center	High (+1)
A	Temperature	°C	45	60	75
B	Time	h	2	3	4
C	Concentration	M	0.2	0.6	1

3. Results and discussion

3.1. Sulfate removal

Sulfate uptake by modified clinoptilolite can be influenced by various operating parameters, including solution concentration, contact time, and temperature during the preparation process. A Box-Behnken experimental design was employed to optimize these factors, as outlined in Table 2.

Experiments were conducted according to the experimental design. As previously mentioned, NaCl-modified clinoptilolite was prepared, and its sulfate removal capabilities were evaluated. Fig. 2 illustrates the sulfate uptake onto the modified Clinoptilolite.

Design-Expert 10 software was used to conduct and analyze the experiments. Runs 1, 3, 5, 6, and 14 were repeated five times based on the Design of experiments (DOE) principles.

The total ion removal efficiency (adsorption efficiency) was calculated using Eq. (1).

$$RE\% = [(C_0 - C_f)/C_0]/\times 100 \quad (1)$$

According to Fig. 2, modification of Clinoptilolite by NaCl has a significantly positive effect on the sulfate adsorption capacity. Runs 1, 3, 4, 6, 7, 8, 9, and 14 of the experiments have the highest adsorption efficiency of around 80%. Runs 1, 3, 5, 6, and 14 are repetitious and are shown by different

Table 2. The experimental design by Box-Behnken.

Run	Factor 1: Temperature (°C)	Factor 2: time (h)	Factor 3: Solution con. (M)	Result efficiency (%)
1	60	3	0.6	81.79574
2	45	4	0.6	47.35413
3	60	3	0.6	80.89046
4	75	3	1	81.58999
5	60	3	0.6	72.98165
6	60	3	0.6	80.75056
7	75	4	0.6	81.25257
8	45	2	0.6	81.73813
9	45	3	1	79.49963
10	75	3	0.2	74.94856
11	75	2	0.6	73.66472
12	60	2	1	75.4012
13	60	4	1	58.94165
14	60	3	0.6	81.7299
15	60	2	0.2	72.98165
16	60	4	0.2	47.35413
17	45	3	0.2	73.66472

textures. All runs (except for Run 5) had good and uniform results.

In RSM, each independent variable is modeled to capture both the main and interaction effects of the factors [1]. RSM establishes an empirical relationship between the response function and the independent variables. This relationship can be approximated using a quadratic polynomial Eq. (2).

$$Y = b_0 + b_1X_1 + b_2X_2 + b_3X_3 + b_{12}X_1X_2 + b_{13}X_1X_3 + b_{23}X_2X_3 + b_{11}X_{21} + b_{22}X_{22} + b_{33}X_{23} \quad (2)$$

The coefficients of the polynomial model are expressed as b_0 (constant expression) and b_1, b_2, b_3 (linear effects), b_{11}, b_{22}, b_{33} (second order effects), and b_{12}, b_{13}, b_{23} (interactive effects) [43].

Using design expert regression software, the coefficients of the response functions for various dependent variables were determined by correlating the experimental data with the response functions [44]. The following quadratic equation was used to model the interactive relationship between removal efficiency (*RE*, %) and the operating parameters in this study.

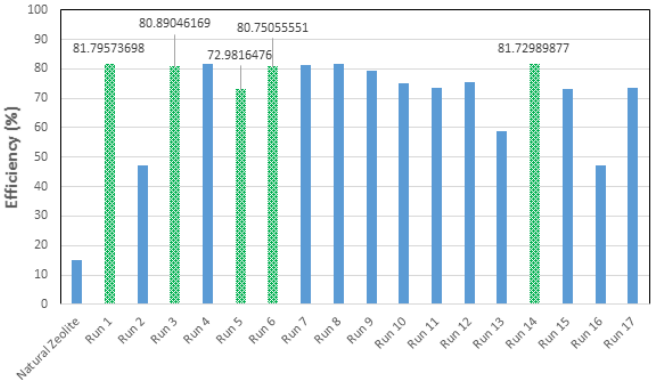

Fig. 2. Results of adsorption experiments based on the Box-Behnken design.

$$Efficiency\ (\%) = 152.91161 - 3.24311 \times (Temp) + 13.12975 \times (time) + 24.83228 \times (Concentration) + 0.69953 \times (Temp) \times (time) + 0.033605 \times (Temp) \times (Concentration) + 5.72998 \times (time) \times (Concentration) + 0.011397 \times (Temp)^2 - 11.19167 \times (time)^2 - 29.80204 \times (Concentration)^2 \quad (3)$$

Analysis of variance (ANOVA) tests the hypothesis that the means of different groups are equal. It partitions the total variance observed in the data into variance due to the treatment (independent variable) and variance due to error (random variation). ANOVA calculates an *F*-statistic, which is the ratio of variance between groups to variance within groups. A high *F*-value indicates that the group means are not all equal, suggesting that at least one group differs significantly from the others. The p-value is derived from the F-statistic calculated in ANOVA. A high F-statistic typically results in a low p-value, indicating significant differences among group means. The *p*-value plays a crucial role in interpreting the results of ANOVA by helping researchers determine the statistical significance of their findings. Hence, ANOVA was employed to assess the interactions between operating parameters and evaluate the overall suitability of the model. All parameters, including adjusted R^2 (Adj-R^2), lack of fit, coefficient of determination *R*-squared (R^2), probability (*p*-value), and Fisher variation ratio (*F*-value), were considered [44].

The *F*-value of the model was 9.99, with a corresponding *p*-value of less than 0.05 (0.0031), indicating the statistical significance of the model's impact on the response [43]. Based on the *F*-values, the operating parameters had the following influential order: time (27.93) > temperature (5.02) > concentration (4.13).

In this case, B, AB, and B^2 are significant model terms. Furthermore, there was no statistically significant interaction among some operating parameters such as (Temp)×(Concentration), (time)×(Concentration), and $(Temp)^2$, since their *p* values were all larger than 0.05.

The lack-of-fit *F* value was found to be 2.2, indicating that the lack of fit was not significantly relative to the pure error. The lack-of-fit results showed that the regression was reasonable (non-significant lack of fit is good). It was evident from these results that the model equations represented the dependence of responses on the independent variables.

More importantly, the square *R* (R^2) equal to 0.9278 and adjusted R^2 equal to 0.8349, which are high and not significantly different, indicate a high reliability of the chosen model. "Adeq Precision" measures the signal-to-noise ratio. A ratio greater than 4 is desirable. In this study, a ratio of 10.809 indicates an adequate signal. This model can be used to navigate the design space. The meaning of coefficient of variation (C.V.) % $\leq$ 10 % is that the model is significant, completely. In this analysis, C.V. is equal to 6.29 %, meaning the results are acceptable (Tables 3 and 4).

Clinoptilolite can be effectively reused after adsorption processes through various regeneration techniques. Research indicates that clinoptilolite can recover a significant portion of its adsorption capacity, making it a viable option for repeated use in applications such as gas capture and wastewater treatment. Furthermore, zeolite wastes derived from other processes can serve as a filler in cement industry or valuable additive in asphalt technology, particularly for warm mix applications, providing benefits related to workability, temperature management, moisture control, and overall performance enhancement [45-47].

Table 4. Analysis of variance (ANOVA) for the quadratic model.

Model	*R*-Squared	Adj *R*-Squared	Adeq precision	C.V. %
Quadratic	0.9278	0.8349	10.809	6.29

3.2. Influence of variables interaction on response (Adsorption efficiency)

Three-dimensional (3D) surface response plots were used to visualize the effects of factor interactions on the response within specific ranges.

Fig. 3 illustrates the influence of temperature and contact time on sulfate removal efficiency. The response surface confirmed the significant impact of time on removal efficiency. Efficiency initially increased but then declined as contact time decreased from 4 to 2 h. The oscillatory trend in the diagram may be attributed to the analysis in Table 3, which indicated that time had a more pronounced effect than concentration and temperature.

Fig. 4 displays the impact of concentration and temperature on sulfate removal percentage. The effect of temperature became less significant as concentration changed, resulting in slower changes in efficiency. Fig. 5 depicts the influence of concentration and time on the adsorptive removal of sulfate by modified clinoptilolite in an aqueous solution. The concentration range was varied from 0.2 to 1 M to assess its

Table 3. ANOVA regression model for sulfate removal by modified clinoptilolite.

Source	Sum of square	Degree of freedom	Mean square	*F*-value	*p*-value	Remark
Model	1909.43	9	212.16	9.99	0.0031	Significant
A- Temp	106.57	1	106.57	5.02	0.0601	
B- Time	593.11	1	593.11	27.93	0.0011	
C- Concentration	87.67	1	87.67	4.13	0.0817	
AB	440.41	1	440.41	20.74	0.0026	
AC	0.16	1	0.16	7.657E-003	0.9327	
BC	21.01	1	21.01	0.99	0.3530	
A^2	27.69	1	27.69	1.30	0.2911	
B^2	527.38	1	527.38	24.83	0.0016	
C^2	95.73	1	95.73	4.51	0.0714	
Residual	148.67	7	21.24			
Lack of fit	92.52	3	30.84	2.20	0.2309	Not significant
Pure Error	56.15	4	14.04			
Cor Total	2058.10	16				

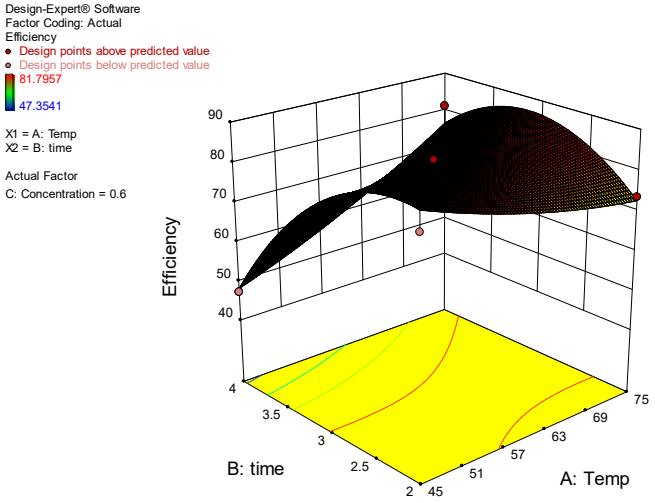

Fig. 3. Three-dimensional response surface plot for the effect of time and temperature during the modification process on the sulfate removal.

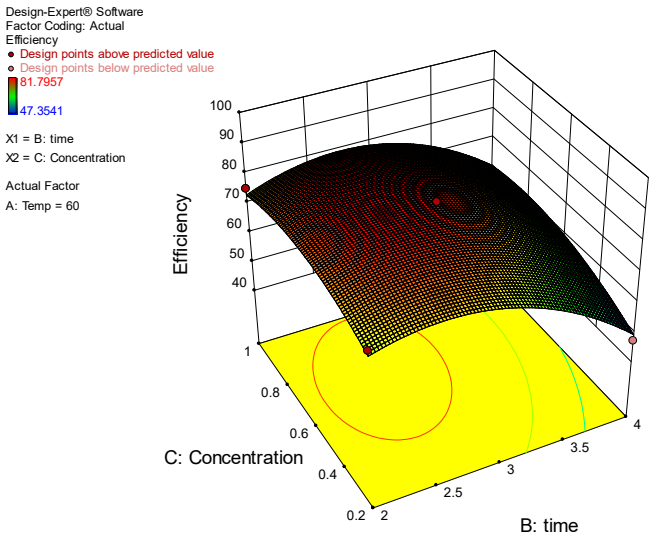

Fig. 5. Three-dimensional response surface plot for the effect of time and concentration during the modification process on the sulfate removal.

impact on sulfate uptake. As demonstrated in Fig. 5, sulfate uptake onto the prepared clinoptilolite samples initially increased with elevation of NaCl solution concentration but then decreased. The changes were gradual, and the effect became more pronounced over time.

3.3. Adsorption capacity

Adsorption capacity refers to the maximum amount of a substance (adsorbate) that can adhere to the surface of an adsorbent material, typically measured in units such as mg of adsorbate per gram of adsorbent (mg.g^{-1}). This property is crucial in various applications, including water treatment, gas purification, and catalysis, where materials are used to remove pollutants or enhance reactions. The adsorption capacity is often determined through experimental methods that involve measuring the concentration of the adsorbate in solution before and after contact with the adsorbent [48,49]. The difference in concentration, along with the volume of solution and mass of the adsorbent, allows for calculating the capacity using formulas like Eq. (4).

$$Q_e = \frac{(C_0 - C_e) \times V}{m} \quad (4)$$

where Q_e is the adsorption capacity (mg.g^{-1} or another appropriate unit), C_0 is the initial concentration of the adsorbate in solution (mg.L^{-1}), C_e is equilibrium concentration of the adsorbate in solution (mg.L^{-1}), V is volume of the solution (L), and m is the mass of the adsorbent (g) [50]. In this study, under the best adsorption conditions, the adsorption capacity is approximately 175 mg.g^{-1}.

There are several effective adsorbents for the removal of sulfate ions from aqueous solutions, each demonstrating varying degrees of efficiency and applicability. Adsorbents for sulfate decontamination can be classified into two types: natural and synthetic. Natural sulfate adsorbents include bioadsorbents and earth compound adsorbents [49,51]. According to the paper topic, the efficiency of some earth-compound adsorbents is compared in Table 5.

Sulfate removal from aqueous solutions on adsorbents involves four main processes: electrostatic attraction, ion exchange, physical adsorption, and hydrogen bonding and complexation. The effectiveness of these mechanisms depends on the type of adsorbent, solution conditions, and the presence of functional groups on the adsorbent. These processes can be enhanced by functional groups. During electrostatic attraction process, due to sulfate ions (SO_4^{2-}) are

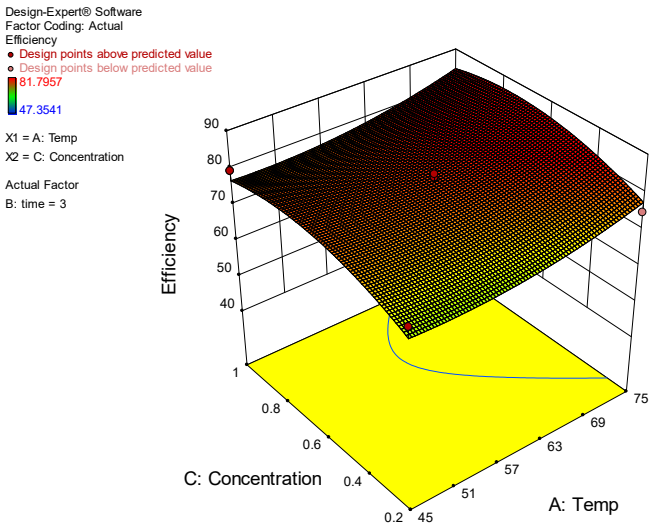

Fig. 4. Three-dimensional response surface plot for the effect of concentration and temperature during the modification process on the sulfate removal.

Table 5. The summary of sulfate adsorption onto earth-compound adsorbents [51].

	Adsorbent	q_{max} (mg.g^{-1})	Ref.
Soil	Andisols	15.36	[53]
	Lateritic soils of west Bengal	0.0246	[54]
Clay	Raw well-ordered Maria III kaolinite (M)	0.86	[55]
	Raw Dunino halloysite (H)	1.74	[55]
Minerals	Natural hematite	4.8	[56]
	Barium-modified zeolite	6.5	[57]
Modified natural zeolite		175	This paper

negatively charged, so they are attracted to positively charged sites on the adsorbent's surface. This attraction is particularly strong if the adsorbent material has functional groups or ions that create a positive surface charge, facilitating the binding of sulfate ions. Zeolites and other modified adsorbents with metal ions often enhance this charge-based attraction [49,51,52].

3.4. X-Ray diffraction (XRD) pattern analysis

In this study, the crystallinity of Clinoptilolite (NZ) and Modified Clinoptilolite (MNZ) adsorbents was estimated using an XRD diffractometer (D8-ADVANCE Bruker, 40 kV, 20 mA, Cu Ka radiation). The average crystallite sizes of the components were estimated by first computing the full width at half-maximum height (FWHM) of the main peaks on the XRD patterns and then using the Debye–Scherrer formula (Eq. (5)).

$$D\,(hkl) = k\lambda / \beta \cos(\theta) \quad (5)$$

where D is average crystallite size (often in nanometers), k is shape factor (depends on the crystallite shape), λ is wavelength of the X-rays used (in nanometers), β is full width at half maximum (FWHM) of the diffraction peak (in radians), and θ is Bragg angle (in radians). The results illustrated that the crystallite sizes of natural zeolite varied between 14.8 and 34.6 nm.

The XRD patterns of clinoptilolite (NZ) and modified clinoptilolite (MNZ) are shown in Figs. 6(A) and (B), respectively. The diffraction peaks observed in the figure are in good agreement with the clinoptilolite structure (JCPDS: 39-1383). The figure's sharp and strong diffraction peaks indicate that the product is well crystallized.

The clinoptilolite in this study showed characteristic peaks at 2θ = 9.931°, 11.25°, 12.17369°, 20.963°, 22.51°, 25.137°, 27.795°, and 29.95°.

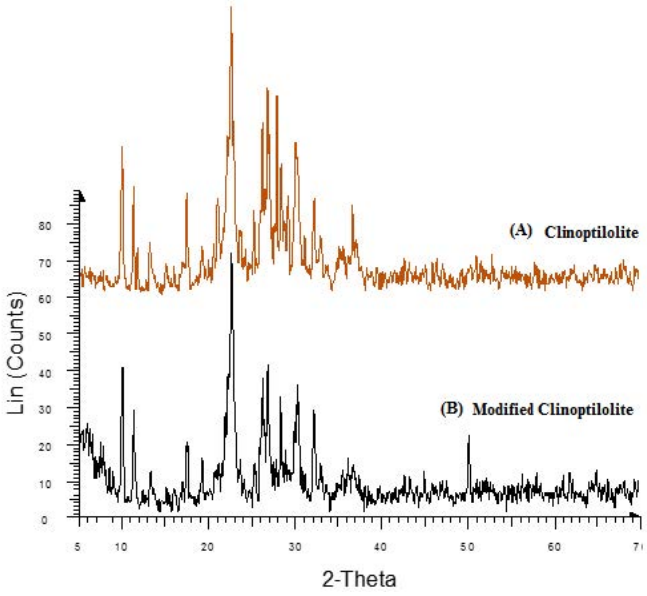

Fig. 6. XRD patterns of clinoptilolite and modified clinoptilolite.

In the XRD spectra of modified clinoptilolite, the diffraction lines are well resolved and it can be observed that the position of the diffraction lines remains constant, revealing that the crystallinity of the original phase was well maintained. Peaks at around 2θ = 28.4°, 32.5°, 46°, 52° in XRD patterns of modified clinoptilolite are related to extra NaCl.

From Fig. 6, it can be seen that the XRD patterns of clinoptilolite used in this work are standard forms of natural zeolite and almost the same as those of modified clinoptilolite, meaning that no crystal form transformation occurred, and the clinoptilolite framework structure was not destructed after clinoptilolite had been modified.

3.5. Energy-dispersive X-ray spectroscopy (EDS) analysis

Figs. 7 and 8 show the EDS analysis of the natural clinoptilolite (NZ) and modified clinoptilolite (MNZ) to investigate the composition of the element's determination, and their weight percentage are shown in Tables 6 and 7.

As is evident in Fig. 7, there are various elements such as O, Na, Mg, Al, Si, K, Ca, and Fe in the clinoptilolite (NZ) and modified clinoptilolite (MNZ) samples with weight percentages of 58.15, 0.7, 0.15, 1.79, 8.23, 0.87, 29.81, and 0.32 %, respectively, for NZ and 58.16, 2.88, 0.2, 6.3, 29.08, 2.8, 0.33 and 0.27 %, respectively, for MNZ. According to the EDS spectra, adding NaCl to (NZ) increased the weight percentage of the Na element from 0.7 to 2.88 %.

3.6. BET Analysis

As shown in Fig. 9, the nitrogen adsorption–desorption isotherms of clinoptilolite show a type IV isotherm with a

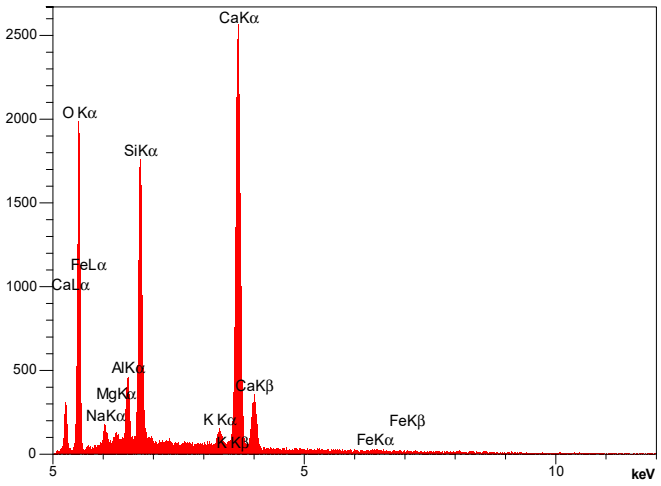

Fig. 7. EDS spectrum of clinoptilolite (NZ).

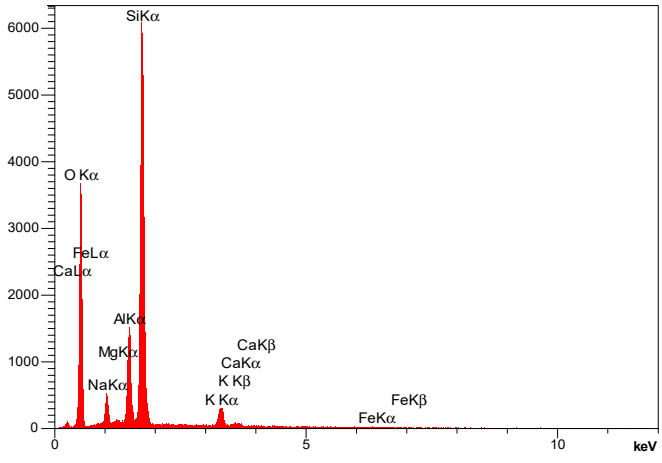

Fig. 8. EDS spectrum of modified clinoptilolite (MNZ).

a hysteresis loop according to the classification of the International Union of Pure and Applied Chemistry (IUPAC). The nitrogen adsorption–desorption isotherms had a larger hysteresis loop at higher relative pressure (P/P_0), suggesting the presence of plentiful mesopores in zeolite [51]. BET analysis demonstrated that the specific surface areas of clinoptilolite, modified clinoptilolite and clinoptilolite after adsorption are 16.56, 19.675, 15.021 $m^2.g^{-1}$, respectively. Furthermore, the total pore volume of clinoptilolite, modified clinoptilolite and clinoptilolite after adsorption are 0.1162, 0.1496, 0.09146 $cm^3.g^{-1}$, respectively. The results show that the particles are well modified and participate well in the adsorption process.

3.7. Fourier-transform infrared spectroscopy analysis

The FT-IR analysis results for functional group determination of modified clinoptilolite in the 400–4000 cm^{-1} range are shown in Fig. 10. The results show that the

Table 6. Weight and atomic percentage of elements of natural clinoptilolite (NZ).

Element	*Wt (%)*	*A (%)*
O	58.15	75.70
Na	0.70	0.63
Mg	0.15	0.13
Al	1.79	1.38
Si	8.23	6.10
K	0.87	0.46
Ca	29.81	15.49
Fe	0.32	0.12
	100.00	100.00

Table 7. Weight and atomic percentage of elements of modified clinoptilolite (MNZ).

Element	*Wt (%)*	*A (%)*
O	58.16	70.98
Na	2.88	2.44
Mg	0.20	0.16
Al	6.30	4.56
Si	29.08	20.21
K	2.80	1.40
Ca	0.33	0.16
Fe	0.27	0.09
	100.00	100.00

spectrum of 3620.14 cm^{-1} is related to the bridging O − H groups in ≡ Al–OH–Si ≡ and are attributed to the location of hydrogen atoms on different oxygen atoms in the framework. The 2979.82 cm^{-1} is related to the Si − OH, the 2513.07 cm^{-1} is related to the Si − N − H stretching vibrations, the 1797.53 cm^{-1} is related to the H − O −H group, the 1182.28 cm^{-1} is related to the Al − O, the 875.62 cm^{-1} is related to the Si (Al) − O, the 798.47 is related to the stretching vibration of Si − O, Al − O in Si − O − Si and Al − O − Al, 711.68 cm^{-1} is related to the O − Si − O, the 611.39 cm^{-1} is related to the tetrahedral double ring oscillations or the vibration of Si – O – M (M = Na, K and Ca), and the 472.53 cm^{-1} is related to the bending of the bonds inside TO4 and symmetric stretching of the free tetrahedral group TO4 (T = Fe, Ti,…), respectively [49,58-61].

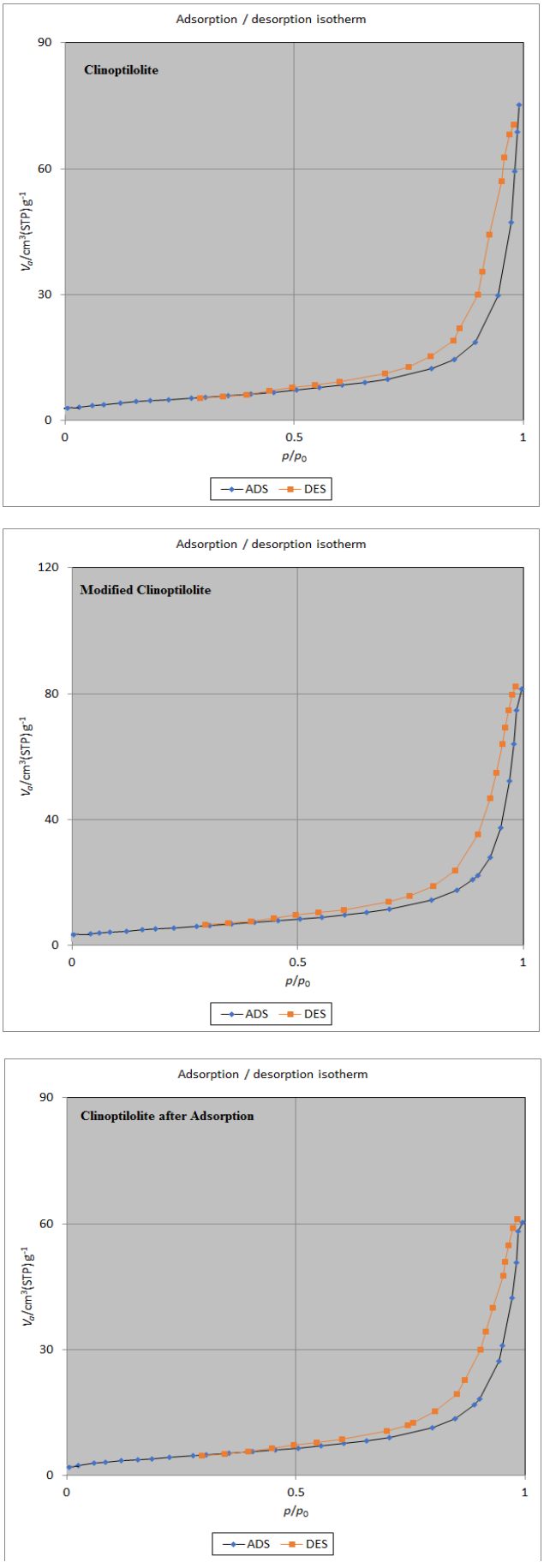

Fig. 9. BET adsorption of natural clinoptilolite, modified cinoptilolite and after adsorption.

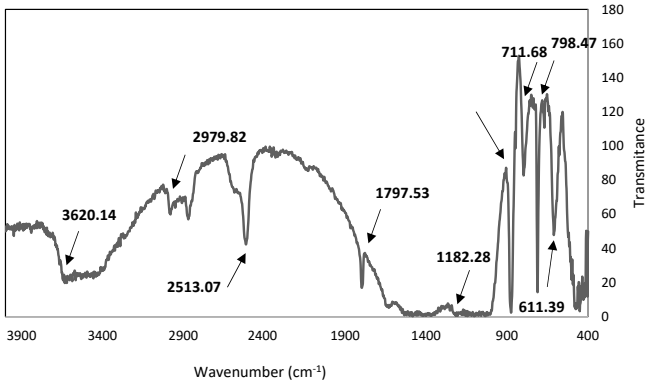

Fig. 10. FT-IR spectrum of modified clinoptilolite (MNZ).

4. Conclusion

This study investigated the adsorption of sulfate ions from aqueous solutions onto modified clinoptilolite. The adsorbent was prepared using a simple, cost-effective method involving NaCl solution and cation exchange. Parameters such as solution concentration, temperature, and contact time were assessed to evaluate the factors influencing adsorbent modification for sulfate removal. Design-Expert software and the Box-Behnken design were employed to identify significant parameters for preparing modified clinoptilolite.

The prepared samples were used for sulfate removal, where adsorption efficiency was evaluated using a batch technique. ANOVA analysis was conducted to elucidate the interaction effects of operating parameters. The results revealed that the highest sulfate ion removal efficiency (81.79 %) occurred at a concentration of 0.6 M, a contact time of 3 h, and a temperature of 60 °C. In general, modified clinoptilolite exhibited high sulfate uptake efficiency. Furthermore, FT-IR, XRD, and EDS analyses were used to characterize the surface properties of the modified clinoptilolite adsorbent.

Conflicts of Interest Statement

The authors certify that they have no affiliations with or involvement in any organization or entity with any financial interest (such as honoraria; educational grants; participation in speakers' bureaus; membership, employment, consultancies, stock ownership, or other equity interest; and expert testimony or patent-licensing arrangements), or non-financial interest (such as personal or professional relationships, affiliations, knowledge or beliefs) in the subject matter or materials discussed in this manuscript.

Disclosure statement

No potential conflict of interest was reported by the authors.

References

[1] Khabazipour, M. & Anbia, M. (2021). Process Optimization and Adsorption Modeling Using Hierarchical Zif-8 Modified with Lanthanum and Copper for Sulfate Uptake from Aqueous Solution: Kinetic, Isotherm and Thermodynamic Studies. *Journal of Inorganic and Organometallic Polymers and Materials, 31*, 2401-2424. https://doi.org/10.1007/s10904-021-01878-6

[2] Krivovichev, V. (2010). *Minerals as Advanced Materials I*, Springer. https://doi.org/10.1007/978-3-540-77123-4

[3] Salami, A., Bonakdari, H., Akhbari, A., Shamshiri, A., Mousavi, F., Farzin, S. Hassanvand, M. & Noori, A. (2020). Performance Assessment of Modified Clinoptilolite and Magneticn Nanotubes on Sulfate Removal and Potential Application in Natural River Samples. *Journal of Inclusion Phenomena and Macrocyclic Chemistry, 97*, 51-63. https://doi.org/10.1007/s10847-020-00982-3

[4] Ma, H., Zhang, J., Wang, M. & Sun, S. (2019). Modification of Y-Zeolite with Zirconium for Enhancing the Active Component Loading: Preparation and Sulfate Adsorption Performance of $ZrO(OH)_2$/Y-Zeolite. *ChemistrySelect, 4*(27), 7981-7990. https://doi.org/10.1002/slct.201901519

[5] Ma, H., Wang, M., Zhang, J. & Su, S. (2019). Preparation Mechanism of Spherical Amorphous $ZrO(OH)_2$/AlOOH Hybrid Composite Beads for Adsorption Removal of Sulfate Radical from Water. *Materials Letters, 247*, 56-59. https://doi.org/10.1016/j.matlet.2019.03.033

[6] Benne, P., Neubert, L., Sperlich, A., & Ernst, M. (2023). Application of a Carbon Dioxide Regenerated Ion-Exchange Process for Removing Sulphate from Drinking Water: A Simple Approach to Estimate Process Performance. *Environmental Science: Water Research & Technology, 9*(3), 973-981. https://doi.org/10.1039/D2EW00655C

[7] Hernández, P., Recio, G., Canales, C., Schwarz, A, Villa-Gomez, D., Southam, G., & Nancucheo, I. (2022). Evaluation of Operating Conditions on Sulfate Reduction from Acidic Wastewater in a Fixed-Bed Bioreactor. *Minerals Engineering, 177*, 107370. https://doi.org/10.1016/j.mineng.2021.107370

[8] Rahmati, M., Yeganeh, G., & Esmaeli, H. (2019). Sulfate Ion Removal from Water Using Activated Carbon Powder Prepared by *Ziziphus Spina-Christi Lotus* Leaf. *Acta Chimica Slovenica, 66*(4), 888-898. https://doi.org/10.17344/acsi.2019.5093

[9] Dehnamaki, S., & Zolgharnein, J. (2022). Sulfate Removal by Barium-Terephthalate MOF Synthesized from Recycled PET-Waste Using Doehlert Design Optimization. *Inorganic Chemistry Communications, 140*, 109388. https://doi.org/10.1016/j.inoche.2022.109388

[10] Zhao, S., Long, Y., Su, Y., Wang, S. Zhang, Z., & Zhang, X. (2021). Cobalt-Enhanced Mass Transfer and Catalytic Production of Sulfate Radicals in MOF-Derived CeO_2•Co_3O_4 Nanoflowers for Efficient Degradation of Antibiotics. *Small, 17*(43), 2101393. https://doi.org/10.1002/smll.202101393

[11] Salehi, S., & Hosseinifard, M. (2020). Optimized Removal of Phosphate and Nitrate from Aqueous Media using Zirconium Functionalized Nanochitosan-Graphene Oxide Composite. *Celloluse, 27*, 8859-8883. https://doi.org/10.1007/s10570-020-03382-5

[12] Castillo, X., Pizarro, J., Ortiz, C., Cid, H., Florez, M.,De Canck, E., & Van Der Voort, P. (2018). A Cheap Mesoporous Silica from Fly Ash as an Outstanding Adsorbent for Sulfate in Water. *Microporous and Mesoporous Materials, 272*, 184-192. https://doi.org/10.1016/j.micromeso.2018.06.014

[13] Ao, H., Cao, W., Hong, Y., Wu, J., & Wei, L. (2020). Adsorption of Sulfate Ion from Water by Zirconium Oxide-Modified Biochar Derived from Pomelo Peel. *Science of the Total Environment, 708*, 135092. https://doi.org/10.1016/j.scitotenv.2019.135092

[14] Ighalo, J. O., Rangabhashiyam, S., Dulta, K., Umeh, C. T., Iwuozor, K. O., Aniagor, C. O., Eshiemogie, S. O., Iwuchukwu, F. U., & Igwegbe, C. A. (2022). Recent Advances in Hydrochar Application for the Adsorptive Removal of Wastewater Pollutants. *Chemical Engineering Research and Design, 184*, 419-456. https://doi.org/10.1016/j.cherd.2022.06.028

[15] Suresh Kumar, P., Korving, L., Keesman, K., van Loosdrecht, M. C. M., & Witkamp, G. (2019). Effect of Pore Size Distribution and Particle Size of Porous Metal Oxides on Phosphate Adsorption Capacity and Kinetics. *Chemical Engineering Journal, 358*, 160-169. https://doi.org/10.1016/j.cej.2018.09.202

[16] Khalid, W., Kui Cheng, C., Lu, P., Tang, J., Liu, X., Ali, A., Shahab, A., & Wang, X. (2022). Fabrication and Characterization of a Novel Ba^{2+}-Loaded Sawdust Biochar Doped with Iron Oxide for the Super-Adsorption of SO_4^{2-} from Wastewater. *Chemosphere, 303*(Part 3), 135233. https://doi.org/10.1016/j.chemosphere.2022.135233

[17] Choi, J., Hong, S.-W., Kimb, D.-J., & Lee, S.-H. (2012). Investigation of Phosphate Removal Using Sulphate-Coated Zeolite for Ion Exchange. *Environmental Technology, 33*(20), 2329-2335. https://doi.org/10.1080/09593330.2012.666569

[18] Salimi, A., Shamshiri, A., Jaberi, E., Bonakdari, H., Akhbari, A., Delatolla, R., Hassanvand, M. R., Agharazi, M., Huang, Y. F., Ahmed, A. N., Elshafie, A. (2022). Total Iron Removal from Aqueous Solution by Using Modified Clinoptilolite. *Ain Shams Engineering Journal, 13*(1),

101495. https://doi.org/10.1016/j.asej.2021.05.009

[19] Wang, S., & Peng, Y. (2010). Natural Zeolites as Effective Adsorbents in Water and Wastewater Treatment. *Chemical Engineering Journal, 156*(1), 11-24. https://doi.org/10.1016/j.cej.2009.10.029

[20] Mercurio, M., Sarkar, B., & Langella, A. (2019). *Modified Clay and Zeolite Nanocomposite Materials*, *Environmental and Pharmaceutical Applications*, Elsevier. https://doi.org/10.1016/C2017-0-01250-8

[21] Król, M.(2020). Natural vs. Synthetic Zeolites. *Crystals, 10*(7), 622. https://doi.org/10.3390/cryst10070622

[22] Zhao, Q., Long, C., Jiang, Z., Yin, W., Tang, A., & Yang, H. (2023). Highly Stable Natural Zeolite/Montmorillonite Hybrid Microspheres with Green Preparation Process for Efficient Adsorption of Ammonia Nitrogen in Wastewater. *Applied Clay Science, 243*, 106787. https://doi.org/10.1016/j.clay.2022.106787

[23] Virpiranta, H., Hermanni Sotaniemi, V., Leiviskä, T., Taskila, S., Rämö, J., Barrie Johnson, D., & Tanskanen, J. (2022). Continuous Removal of Sulfate and Metals from Acidic Mining-Impacted Waters at Low Temperature Using a Sulfate-Reducing Bacterial Consortium. *Chemical Engineering Journal, 427*, 132050. https://doi.org/10.1016/j.cej.2021.132050

[24] Zhu, M., Tan, Z., Ji, X., & He, Z. (2022). Removal of Sulfate and Chloride Ions from Reverse Osmosis Concentrate Using a Two-Stage Ultra-High Lime with Aluminum Process. *Journal of Water Process Engineering, 49*, 103033. https://doi.org/10.1016/j.jwpe.2022.103033

[25] Li, H., Chai, L., Cui, J., Zhang, F., Wang, F., & Li, S. (2022). Polypyrrole-Modified Mushroom Residue Activated Carbon for Sulfate and Nitrate Removal from Water: Adsorption Performance and Mechanism. *Journal of Water Process Engineering, 49*, 102916. https://doi.org/10.1016/j.jwpe.2022.102916

[26] Guerrero-Flores, A. D., Elizondo Alvarez, M. A., Flores Alvarez, J. M., & Uribe-Salas, A. (2022). Comparative Study on Simultaneous Removal of Calcium and Sulfate Ions from Flotation Recycling Water by Aluminum Hydroxide. *Transactions of Nonferraous Metals Society of China, 32*(7), 2379-2390. https://doi.org/10.1016/S1003-6326(22)65954-5

[27] Moreroa-Monyelo, M., Falayi, T., Ntuli, F., & Magwa, N. (2022). Studies Towards the Adsorption of Sulphate Ions from Acid Mine Drainage by Modified Attapulgite Clays. *South African Journal of Chemical Engineering, 42*, 241-254. https://doi.org/10.1016/j.sajce.2022.08.011

[28] Voutetaki, A., Plakas, K. V., Papadopoulos, A. I., Bollas, D., Parcharidis, S., & Seferlis, P. (2023). Pilot-Scale Separation of Lead and Sulfate Ions from Aqueous Solutions Using Electrodialysis: Application and Parameter Optimization for the Battery Industry. *Journal of Cleaner Production, 410*, 137200. https://doi.org/10.1016/j.jclepro.2023.137200

[29] Chatla, A., Almanassra, I. W., Abushawish, A., Laoui, T., Alawadhi, H., Atieh, M. A., & Ghaffour, N. (2023). Sulphate Removal from Aqueous Solutions: State-of-the-Art Technologies and Future Research Trends. *Desalination, 558*, 116615. https://doi.org/10.1016/j.desal.2023.116615

[30] Zhou, X., Fernández-Palacios, E., Dorado, A. D., Lafuente, J., Gamisans, X. & Gabriel, D. (2024). The Effect of Slime Accumulated in a Long-Term Operating UASB Using Crude Glycerol to Treat S-Rich Wastewater. *Journal of Environmental Sciences, 135*, 353-366. https://doi.org/10.1016/j.jes.2022.11.011

[31] Pratinthong, N., Sangchan, S., Chimupala, Y., & Kijjanapanich, P. (2021). Sulfate Removal from Lignite Coal Mine Drainage in Thailand Using Ettringite Precipitation. *Chemosphere, 285*, 131357. https://doi.org/10.1016/j.chemosphere.2021.131357

[32] Qin, C., Yao, D., Cheng, C., Xie, H., Hu, Z., & Zhang, J. (2022). Influence of Iron Species on the Simultaneous Nitrate and Sulfate Removal in Constructed Wetlands Under Low/High COD Concentrations. *Environmental Research, 212*(Part C), 113453. https://doi.org/10.1016/j.envres.2022.113453

[33] Kennedy, D. A., Mujčin, M., Abou-Zied, C., & Tezel, F. H. (2019). Cation Exchange Modification of Clinoptilolite –Thermodynamic Effects on Adsorption Separations of Carbon Dioxide, Methane, and Nitrogen. *Microporous and Mesoporous Materials, 274*, 327-341. https://doi.org/10.1016/j.micromeso.2018.08.035

[34] Kennedy, D. A., & Tezel, F. H. (2018). Cation Exchange Modification of Clinoptilolite - Screening Analysis for Potential Equilibrium and Kinetic Adsorption Separations Involving Methane, Nitrogen, and Carbon Dioxide. *Microporous and Mesoporous Materials, 262*, 235-250. https://doi.org/10.1016/j.micromeso.2017.11.054

[35] Price, L. A., Jones, Z., Nearchou, A., Stenning, G., Nye, D., & Sartbaeva, A. (2022). The Effect of Cation Exchange on the Pore Geometry of Zeolite L. *AppliedChem, 2*(3), 149-159. https://doi.org/10.3390/appliedchem2030011

[36] Campanile, A., Liguori, B., Ferone, C., Caputo, D. & Aprea, P. (2022). Zeolite-Based Monoliths for Water Softening by Ion Exchange/Precipitation Process. *Scientific Reports, 12*, 3686. https://doi.org/10.1038/s41598-022-07679-2

[37] Łach, M., Grela, A., Pławecka, K., Duarte Guigou, M., Mikuła, J., Komar, N., Bajda, T., & Korniejenko, K. (2022). Surface Modification of Synthetic Zeolites with Ca and HDTMA Compounds with Determination of

Their Phytoavailability and Comparison of CEC and AEC Parameters. *Materials, 15*(12), 4083. https://doi.org/10.3390/ma15124083

[38] Antony, J. (2014). *Design of Experiments for Engineers and Scientists*, Elsevier. https://doi.org/10.1016/C2012-0-03558-2

[39] Shojaei, S., Shojaei, S., & Pirkamali, M. (2019). Application of Box–Behnken Design Approach for Removal of Acid Black 26 from Aqueous Solution Using Zeolite: Modeling, Optimization, and Study of Interactive Variables. *Water Conservation Science and Engineering, 4*, 13-19. https://doi.org/10.1007/s41101-019-00064-7

[40] Oyinade, A., SanniKovo, A., & Hill, P. (2016). Synthesis, Characterization and Ion Exchange Isotherm of Zeolite Y Using Box–Behnken Design. *Advanced Powder Technology, 27*(2), 750-755. https://doi.org/10.1016/j.apt.2016.03.002

[41] Mehdi, B., Belkacemi, H., Brahmi-Ingrachen, D., AitBraham, L., & Muhr, L. (2022). Study of Nickel Adsorption on Nacl-Modified Natural Zeolite Using Response Surface Methodology and Kinetics Modeling. *Groundwater for Sustainable Development, 17*, 100757. https://doi.org/10.1016/j.gsd.2022.100757

[42] Li, M., Feng, C., Zhang, Z., Chen, R., Xue, Q., Gao, C., & Sugiura, N. (2010). Optimization of Process Parameters for Electrochemical Nitrate Removal Using Box–Behnken Design. *Electrochimica Acta, 56*(1), 265-270. https://doi.org/10.1016/j.electacta.2010.08.085

[43] Afshin, S., Rashtbari, Y., Vosough, M., Dargahi, A., Fazlzadeh, M., Behzad, A., Yousefi, M. (2021). Application of Box–Behnken Design for Optimizing Parameters of Hexavalent Chromium Removal from Aqueous Solutions Using Fe_3O_4 Loaded on Activated Carbon Prepared from Alga: Kinetics and Equilibrium Study. *Journal of Water Process Engineering, 42*, 102113. https://doi.org/10.1016/j.jwpe.2021.102113

[44] Nguyen, D. T. C., Vo, D. V. N., Nguyen, C. N. Q., Ai Pham, L. H., Le, H. T. N., Nguyen, T. T. T., & Tran, T. V. (2021). Box–Behnken Design, Kinetic, and Isotherm Models for Oxytetracycline Adsorption onto Co-Based ZIF-67. *Applied Nanoscience, 11*, 2347-2359. https://doi.org/10.1007/s13204-021-01954-w

[45] Jiang, B., Zhang, B., Duan, X. & Xing, Y. (2024). CO_2 Capture by Modified Clinoptilolite and Its Regeneration Performance. *International Journal of Coal Science & Technology, 11*, 20. https://doi.org/10.1007/s40789-023-00661-x

[46] Sol-Sanchez, M., Moreno-Navarro, F., Rubio-Gámez, M. C., Pérez-Mena, V., & Cabanillas, P. (2019). Reuse of Zeolite By-Products Derived from Petroleum Refining for Sustainable Roads. *Advances in Materials Science and Engineering, 2019*, 4256989. https://doi.org/10.1155/2019/4256989

[47] Li, Z., Ren, J., Zhu, J., Li, W., Fu, Z., & Yang, L. (2020). Study on the Construction Performance of Zeolite Asphalt Mixture Based on Macro-Micro Scale. *Advances in Materials Science and Engineering, 2020*, 4137321. https://doi.org/10.1155/2020/4137321

[48] Qi, X., Tong, X., Pan, W., Zeng, Q., You, S., & Shen, J. (2021). Recent Advances in Polysaccharide-Based Adsorbents for Wastewater Treatment. *Journal of Cleaner Production, 315*, 128221. https://doi.org/10.1016/j.jclepro.2021.128221

[49] Sadeghalvad, B., Ahali, Z., & Azadmehr, A. (2016). Modification of Natural Zeolite by Carboxylate Compounds and Minerals for Removal of Zinc Ions from Wastewater: Equilibrium and Kinetic Studies. *Arabian Journal for Science and Engineering, 41*, 2501-2513. https://doi.org/10.1007/s13369-015-2003-4

[50] Yang, X., Zhang, H., Cheng, S., & Zhou, B. (2022). Optimization of the Adsorption and Removal of Sb(III) by MIL-53(Fe)/GO Using Response Surface Methodology. *RSC Adv, 12*, 4101-4112. https://doi.org/10.1039/D1RA08169A

[51] Sadeghalvad, B., Khorshidi, N., Azadmehr, A., & Sillanpää, M. (2021). Sorption, Mechanism, and Behavior of Sulfate on Various Adsorbents: A Critical Review. *Chemosphere, 263*, 128064. https://doi.org/10.1016/j.chemosphere.2020.128064

[52] Tian, B., Song, Y., Wang, R., Wang, Y., Wang, T., Chu, J., Qiao, Z., Li, M., Lu, J., & Tong, Y. (2023). Adsorption of Sulfate Ions from Water by $CaCl_2$-Modified Biochar Derived from Kelp. *RSC Sustainability, 1*, 898-913. https://doi.org/10.1039/D2SU00136E

[53] Pigna, M., & Violante, A. (2003). Adsorption of Sulfate and Phosphate on Andisols. *Communications in Soil Science and Plant Analysis, 34*(15-16), 2099-2113. https://doi.org/10.1081/CSS-120024051

[54] Ghosh, G. K., & Dash, N. R. (2012). Sulphate Sorption-Desorption Characteristics of Lateritic Soils of West Bengal, India. *International Journal of Plant, Animal and Environmental Sciences, 2*(1), 167-176.

[55] Matusik, J. (2014). Arsenate, Orthophosphate, Sulfate, and Nitrate Sorption Equilibria and Kinetics for Halloysite and Kaolinites with an Induced Positive Charge. *Chemical Engineering Journal, 246*, 244-253. https://doi.org/10.1016/j.cej.2014.03.004

[56] Sadeghalvad, B., Azadmehr, A., & Hezarkhani, A. (2016). Assessment of Iron Ore Mineral Wastes for Sulfate Removal from Groundwater Wells: A Case Study. *RSC Advances, 6*(14), 11719-11734. https://doi.org/10.1039/C5RA21843H

[57] Runtti, H., Tynjälä, P., Tuomikoski, S., Kangas, T., Hu, T., Rämö, J., & Lassi, U. (2017). Utilisation of Barium-Modified Analcime in Sulphate Removal: Isotherms, Kinetics and Thermodynamics Studies. *Journal of Water Process Engineering, 16*, 319-328. https://doi.org/10.1016/j.jwpe.2016.11.004

[58] Ruiz-Serrano, D., Flores-Acosta, M., Conde-Barajas, E., Ramírez-Rosales, D., Yáñez-Limón, J., & Ramírez-Bon, R. (2010). Study by XPS of Different Conditioning Processes to Improve the Cation Exchange in Clinoptilolite. *Journal of Molecular Structure, 980*(1-3), 149-155. https://doi.org/10.1016/j.molstruc.2010.07.007

[59] Pavia, D., Lampman, G., Kriz, G., & Vyvyan, J. (2015). *Introduction to Spectroscopy*, Cengage Learning, 5th ed.

[60] Gauglitz, G., & Moore, D. S. (2014). *Handbook of Spectroscopy*, 2nd, Enlarged Edition, Wiley-VCH Verlag GmbH & Co. https://doi.org/10.1002/9783527654703

[61] Chaudhary, J., Tailor, G., Yadav, M., & Mehta, C. (2023). Green Route Synthesis of Metallic Nanoparticles Using Various Herbal Extracts: A Review. *Biocatalysis and Agricultural Biotechnology, 50*, 102692. https://doi.org/10.1016/j.bcab.2023.102692

Additional information

Correspondence and requests for materials should be addressed to K. Peyvandi.

HOW TO CITE THIS ARTICLE

Hematian, S.; Peyvandi, K.; Enhanced sulfate removal from aqueous solution using ion-exchanged clinoptilolite: A study on adsorption efficiency and process optimization*, J. Part. Sci. Technol. **(*) **-**.*

DOI: 10.22104/jpst.2024.7130.1264
URL: https://jpst.irost.ir/article_1471.html